

“Live” Prussian blue fading by time-resolved X-ray absorption spectroscopy

Claire Gervais · Marie-Angélique Languille ·
Solemn Reguer · Martine Gillet · Edward P. Vicenzi ·
Sébastien Chagnot · François Baudelet · Loïc Bertrand

Received: 3 August 2012 / Accepted: 20 January 2013 / Published online: 30 January 2013
© Springer-Verlag Berlin Heidelberg 2013

Abstract Prussian blue (PB) is an artists’ pigment that has been frequently used in many artworks but poses several problems of conservation because of its fading under light and anoxia treatment. PB fading is due to the reduction of iron(III) into iron(II) and depends a lot on the object investigated. Due to the complexity of the structure, the precise physico-chemical mechanisms behind the redox process remain obscure. In this paper, we present a procedure to investigate light- and anoxia-induced fading of PB-paper samples

by means of time resolved X-ray absorption spectroscopy performed at the Fe K-edge. A system composed of a visible light source and a flux-controlled environmental cell allowed light, gas and humidity to be modified in situ. The synchrotron X-ray beam was evidenced to induce a reduction of PB and to play a major role in the kinetics. The analysis of the PB fading kinetics of a sample submitted to various gas and light environments showed that both synchrotron beam and anoxia were influencing PB reduction in a correlated way. In comparison, light was found to play a minor role. Finally, we have demonstrated that the type of paper substrate could influence significantly the kinetics of reduction. Several hypotheses to explain the correlation between PB reduction mechanism and substrate are presented.

C. Gervais (✉) · E.P. Vicenzi
Smithsonian Institution Museum Conservation Institute,
4210 Silver Hill Road, Suitland, MD 20746, USA
e-mail: claire.gervais@hkb.bfh.ch

Present address:

C. Gervais
Bern University of the Arts, Fellerstrasse 11, 3027 Bern,
Switzerland

M.-A. Languille · L. Bertrand
IPANEMA, USR 3461 CNRS/MCC, Synchrotron SOLEIL,
BP48 Saint-Aubin, 91192 Gif-sur-Yvette, France

L. Bertrand
Synchrotron SOLEIL, BP48 Saint-Aubin, 91192 Gif-sur-Yvette,
France

S. Reguer
DiffAbs beamline, Synchrotron SOLEIL, BP48 Saint-Aubin,
91192 Gif-sur-Yvette, France

M. Gillet
Centre de Recherche sur la Conservation des Collections,
Muséum national d’histoire naturelle, 36 rue Geoffroy
Saint-Hilaire CP 21, 75005 Paris, France

S. Chagnot · F. Baudelet
ODE beamline, Synchrotron SOLEIL, BP48 Saint-Aubin,
91192 Gif-sur-Yvette, France

1 Introduction

Prussian blue (PB, iron(III) hexacyanoferrate(II)) is a pigment widely used in Europe in the 18th and 19th centuries. Synthesized accidentally in 1706 by the colormaker Diesbach, the pigment was used as early as 1710 by painters [1] and was later employed in the first photographic printing processes [2], as a dye, and for a wide range of manufactured objects (e.g., blueprints, stamps, etc.). Cultural objects composed of Prussian blue pose several problems of conservation, among which their sensitivity to the environment. When exposed to visible light, PB artefacts partly discolor due to the photoreduction of iron(III) into iron(II). PB may also fade when submitted to anoxic treatment, a method often employed to eradicate insect infestations, raising concern among conservators about the validity of such a method for treating PB-containing objects [3]. In both cases, the amount of PB fading and its kinetics are correlated and depend strongly of the object investigated, making difficult the

establishment of a general preventive conservation procedure.

The crystalline structure of PB consists in a cubic lattice occupied by $\text{Fe}^{\text{II}}\text{-C}\equiv\text{N-Fe}^{\text{III}}$ building blocks [4, 5]. A charge transfer via the cyano group occurs around ~ 640 nm and is responsible for the blue color of the pigment. Despite this apparent simplicity, the structure of PB and PB analogues (where iron is substituted by similar transition metal atoms [6]) is complex and contains Fe(II) vacancies, interstitial cations and a complex water network [7, 8]. These structural features play a decisive role on the final magnetic, optical and redox properties of the compounds [9–11], making Prussian blue a class of compounds still abundantly investigated for various promising applications such as memory devices, magneto-optical switches and biosensors [12, 13].

Our aim is to further investigate the relationships between the structure of PB and its redox and optical properties, however in the context of PB-containing cultural objects. By deciphering the exact physico-chemical processes responsible for light-induced and anoxia-induced PB reduction, we hope to rationalize the versatility of PB fading in cultural artefacts and give to conservators sufficient knowledge to design adequate conservation solutions to mitigate PB fading. In this context, recent studies based on X-ray Absorption Near Edge Spectroscopy (XANES) at the Fe K-edge of PB-paper samples have shown that light-induced fading is a complex mechanism, which cannot be simply restricted to a reduction of Fe(III) to Fe(II) [8, 14]. Particularly, the influence of the substrate has been evidenced to play a major role on the structural changes happening during light-induced fading [8]. As well, the influence of the anoxic environment on PB fading has been tackled recently [15, 16], but much work remains to be done to understand precisely the structural changes happening upon anoxia-induced fading and compare the relative capability of light and anoxia to discolor Prussian blue.

We present here a procedure based on energy-dispersive X-ray Absorption Spectroscopy (XAS) experiments at the Fe K-edge to follow in situ the fading of PB deposited on different substrates and subjected to light and anoxia treatments. This work aims at highlighting the influence of (i) the type of fading (anoxia vs light) and (ii) the type of substrate on the overall physico-chemical process taking place during fading. We first present the data processing applied to estimate the fading kinetics and show that this procedure yields reproducible results. In a second part, the procedure is applied onto a sample submitted to different gas environments, and we discuss the impact of light, anoxia and synchrotron beam exposure on the reduction of Prussian blue. In a third part, the variations of fading kinetics due to the substrate are presented and discussed. Possible routes to investigate further Prussian blue fading conclude this paper.

2 Experimental details

2.1 Samples

The samples studied here are Prussian blue colored papers, for which the fading behavior and some structural data have already been collected. Soluble Prussian blue was produced following the synthesis developed by Dostal et al. [17]. Two papers with very different light stabilities were chosen in order to investigate the influence of the substrate oxidation properties on Prussian blue fading [8]: *Whatman* paper is a 100 % cellulose neutral paper often used as a reference paper in conservation for its relative stability. *Step3* contains 25 % lignin, several fillers and exhibit an acidic pH ($\text{pH} = 5.4$). It yellows readily and is very sensitive to light exposure. *Whatman* and *Step3* were immersed into a colloidal aqueous solution of Prussian blue (125 mg in 1 mL of deionized water) and were left to dry at room temperature and ambient humidity (40 % RH). When dried, the colored papers were mounted into the controlled atmosphere cell.

2.2 Controlled atmosphere

A controlled atmosphere flow cell was specifically designed in order to work in transmission geometry through two Mylar windows (30 μm) transparent to X-rays at the Fe K-edge (see Fig. 1). The cell works at atmospheric pressure of neutral gas. The internal volume (8 cm^3) is relatively large comparing to the sample size (14 \times 4 mm^2) and the cell. Moreover, the continuous gas flux allows an equilibrium of gas composition and relative humidity between the sample and the internal volume. Humidity and temperature are continuously monitored at the exit of the cell using a thermo-hygrometer. Two environments were chosen: air-50 % RH and N_2 -50 % RH, hereafter referred as *Air* and *Anoxia*, respectively. The entire system (gas system + cell) was allowed to equilibrate for several hours prior mounting the sample. After mounting, the system was again equilibrated for 15 minutes (until stabilization of the hygrometry at the exit of the cell) prior measurement. The sample could be simultaneously illuminated with a focused visible Xe source of 0.4 mm diameter. The luminance was measured to be 1.5 MLux onto the surface of the sample, a power able to reproduce an accelerating fading [18]. Hereafter, *Light* and *Dark* designate experiments performed under light and no light, respectively.

2.3 Dispersive XAS for kinetic measurements

The X-ray absorption spectroscopy measurements have been performed at the ODE beamline of the SOLEIL synchrotron [19]. ODE is a bending magnet beamline fully dedicated to dispersive XAS experiments. A polychromatic

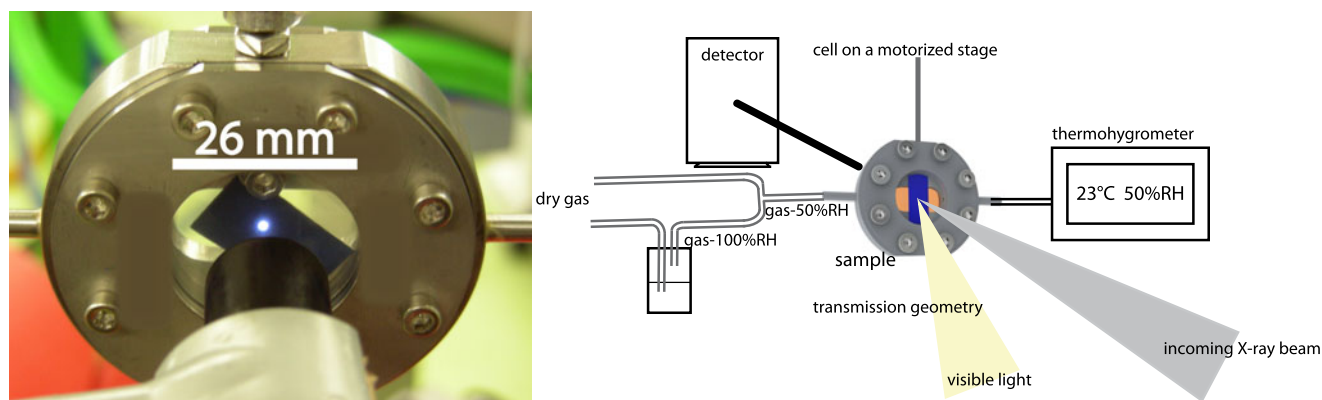


Fig. 1 Experimental setup to monitor in situ anoxia- and light-induced fading of Prussian blue. *Left*: photograph showing the exposure to visible light of a PB–paper sample conditioned in the custom environmental cell. *Right*: Sketch of the experimental setup highlighting the system used to obtain a constant gas flux through the cell. Relative humidity can be modified by two valves regulating the outputs of dry

gas and 100 % RH humidified gas obtained by letting the gas bubbling in distilled water. The light source is facing the sample while the X-ray beam is positioned at 45-degree angle. Positioning of the light to focus at the same location onto the sample than the synchrotron beam was performed with the help of X-ray photography paper

beam is selected with a curved polychromator and focused onto the sample. The divergent beam is detected after the sample on a CCD camera, where the beam position is correlated to energy. The detection of all the energies at the same time allow dispersive XAS to acquire spectra very rapidly (few μs). To perform in-situ light-fading experiments, the visible light source was set to face the sample, at a position of 45-degree angle relative to the X-ray beam (see Fig. 1). The size of the X-ray beam was around $30\ \mu\text{m}$ FWHM in horizontal and $35\ \mu\text{m}$ FWHM in vertical, whereas the visible light was focused on a $0.13\ \text{mm}^2$ area. Spectra were recorded in transmission geometry at the Fe K-edge at room temperature. The energy range of the XAS spectra was $\sim 425\ \text{eV}$. The CCD exposure time was chosen from 5 to 25 ms depending on the pigment concentration into the samples. Up to 150 successive exposures (frames) were saved and averaged to get the final XAS spectrum. Spectra were recorded every 30 s. Due to sample intrinsic heterogeneities, an oscillating movement of the sample over $200\ \mu\text{m}$ in horizontal and vertical was performed during acquisition of the 150 frames. This allowed the final spectrum to be averaged over an area larger than the initial beam spot size. The CCD camera was regularly exposed to the direct beam to record the I_0 spectrum. The spectrum of a metallic iron foil was also regularly recorded during the measurements and used for energy calibration based on the inflection point of the absorption edge at $7112\ \text{eV}$. This calibration was then applied to the spectra of PB-samples. Data treatment was performed using the Iffefit 3.0.3 package with the computational code Athena [20]. The pre-edge range background was removed using an empirical Victoreen function (polynomial), and the absorption background was removed using a cubic spline with a normalisation range between 40 and $220\ \text{eV}$ after the edge.

3 Results and discussion

3.1 Procedure to estimate the kinetics of fading

Typical XAS variations observed upon fading While small variations in the signal evidence for the variability of the structure with synthesis, environmental conditions and substrate, the XAS spectrum of Prussian blue exhibits typical features that may be summarized hereafter: (i) The absorption edge is broad and accounts for the different Fe(II) and Fe(III) environments in the cubic structure; (ii) The weak or absence of EXAFS signal is due to a strong multiple scattering of the $\text{Fe}^{\text{II}}\text{-C}\equiv\text{N-Fe}^{\text{III}}$ building blocks [21]; (iii) Two prepeaks may be theoretically observed, but their intensity is weak because of the octahedral coordination of Fe ions.

XAS spectra observed on the ODE beamline follow this scheme, however with a supplementary contribution to the signal in the form of a low-intensity sinusoid shape visible especially after the edge (Fig. 2a). These oscillations could be due to the defects of the beamline optics. This supplementary contribution, which is normally compensated by the ratio I_{trans}/I_0 when calculating the absorption signal, $\ln(I_{\text{trans}}/I_0)$, cannot be compensated in the present case due to the porosity of the PB sample. Indeed, in the case of diffusing samples, such as zeolites, porous materials and here colored paper with Prussian blue, photons get scattered while passing through the sample, so that identical oscillations are not present in I_{trans} and I_0 .

Variations of the spectra upon fading consist principally in a shift of the absorption edge toward lower energies, accounting for the reduction of Fe(III) into Fe(II). In addition, the intensities of the absorption edge decrease, and the prepeaks increase respectively, due to a disorder and deformation of the octahedral coordination sphere of the Fe ions.

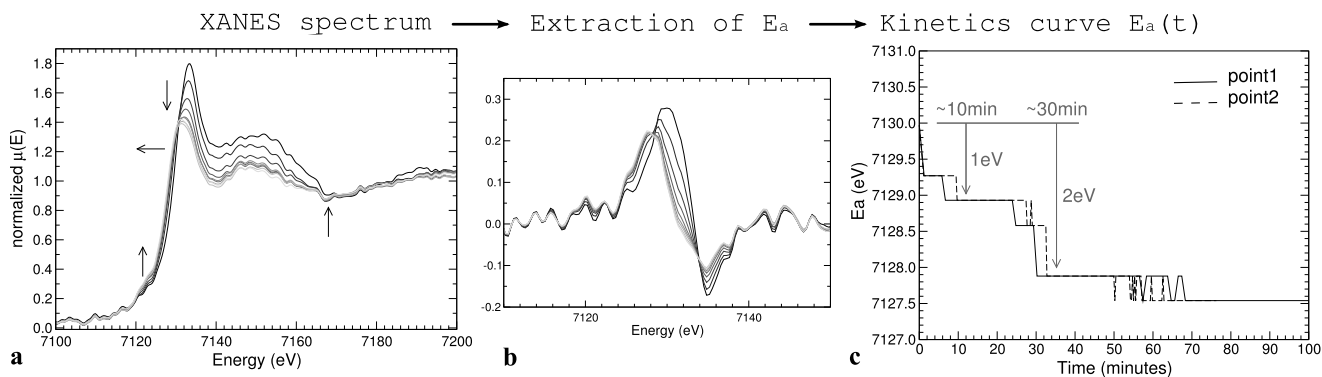


Fig. 2 Procedure to estimate the kinetics of Prussian blue fading from XANES data. Sample: PB-*Whatman* sample in *Anoxia-Light* environment. **(a)** Time evolution of XANES spectra. Arrows indicate major changes with time. **(b)** The derivatives of the spectra are calculated. The maximum of the derivative defines E_a . **(c)**: Final kinetics curve

$E_a(t)$ used to estimate the fading kinetics. *Solid and dashed curves* correspond to two measurements on the same sample. In **(a)** and **(b)**: Only spectra obtained every 10 minutes are shown. Grayscale ranges from black ($t = 0$ min) to light gray ($t = 90$ min)

Note also an immediate decrease in intensity of the spectrum at 7168 eV, which remains invariant after 10 minutes (see arrow Fig. 2a). This feature is interesting but was however not observable in all samples and environmental conditions.

Visualization of the fading kinetics To follow and compare the fading behavior of the different samples, we looked at the variation upon time of the energy at the absorption edge. Note that the prepeak region is also traditionally used to monitor redox kinetics [22]. However, for most of our samples, this region was too noisy to be reliably processed. The energy at the absorption edge was defined as the inflection point of the white line and was extracted by measuring the energy E_a at the maximum of the signal derivative (Fig. 2b). E_a was then plotted against time to give a final estimate of the kinetics $E_a(t)$ (Fig. 2c). The extent of fading (total energy variation, ΔE_a) can also be derived from the kinetics.

The reproducibility of the measurements was tested by monitoring the fading kinetics on two different locations of the same sample. As can be observed in Fig. 2c, both kinetics curves are identical, confirming the reproducibility of the entire procedure. Typical information that can be extracted from Fig. 2c is that the sample fades very rapidly (-1 eV after a few minutes) and stabilizes at $\Delta E_a = -2$ eV after 30 min.

Reducing the entire absorption signal to E_a neglects subtle structural changes that could arise at other energies of the spectrum. However, such a one-point measure gives a reasonable estimate of the iron reduction in PB (which generally induces a shift of the absorption edge) and thus of the fading of the pigment. Nevertheless, we always checked the XANES spectral evolution as a function of time, in order to avoid relying uniquely on the kinetic curves for interpreting the fading behaviors.

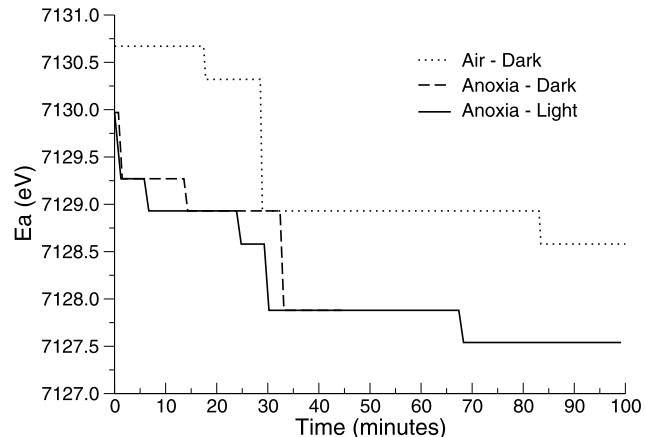


Fig. 3 $E_a(t)$ for PB-*Whatman* sample in three different environments. For clarity, only one kinetics curve out of two is shown for each environment, and the data points have been reduced to feature only the times where E_a changes

3.2 The multiple sources of fading

Influence of the environment on the fading kinetics To estimate the contribution of light, anoxia and synchrotron beam (hereafter SR beam) to the fading of Prussian blue, the kinetics $E_a(t)$ for PB-*Whatman* samples was investigated in *Anoxia-Dark* and *Air-Dark* in addition to the *Anoxia-Light* environment already presented (Fig. 3).¹

First, a reduction is observed in *Air-Dark* (Fig. 3, dotted line), although visual and colorimetric measurements of similar samples confirm that this system should be stable in normal conditions. Therefore, the SR microfocused beam reduces also Prussian blue and must be considered as a third

¹Unfortunately, the kinetics experiments performed on samples in *Air-Light* environment were discarded because of problems with light focus.

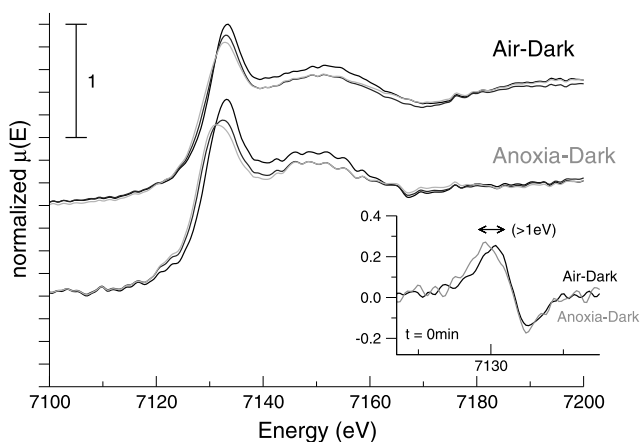


Fig. 4 XANES spectra for PB-Whatman samples in *Air-Dark* and *Anoxia-Dark* environments. *Anoxia-Dark* spectra were shifted in intensity for more clarity. Exposure times: $t = 0$ min (black), $t = 20$ min (dark gray), $t = 50$ min (light gray). *Insert*: XANES signal derivatives at time $t = 0$ min

possible source of fading beside light and anoxia. Second, the PB kinetics in *Anoxia-Light* and *Anoxia-Dark* are very similar (Fig. 3, plain and dashed lines). In both cases, a drop of $\Delta E_a = -2$ eV is observed after 30 min. Therefore, the fading kinetics of *Anoxia* samples do not seem to depend on light exposure. Finally, *Anoxia* samples have a lower starting E_a value than *Air* sample, and a drop of ~ 1 eV happens the first minutes. These differences are also directly observed on the XANES spectra (Fig. 4): a shift of the absorption edge of ~ 1 eV is already observed between the initial spectra of *Anoxia* and *Air* samples, and this difference continues to be visible all along the measurement. Besides, an increase of the prepeak not visible in *Air* happens for *Anoxia* samples.

The impact of anoxia is complex and correlated with SR beam damage

From these observations we conclude that: (i) the SR beam itself is a major source of PB reduction, and (ii) anoxia plays a noticeable role on the fading process. The precise correlation between these two factors remains however somewhat complex. Considering the shift of the absorption edge observed at $t = 0$ min for *Anoxia* samples compared to *Air* samples (see Fig. 3 at $t = 0$ and Fig. 4, insert), it seems that the impact of anoxia on the oxydation state of PB happens immediately (note that samples were in anoxic environment *before* the start of the experiment). Anoxia is thus inherently a reducer, even in the absence of light or SR beam damage.²

²The total exposure time to measure one XANES spectrum is 20.3 s for an average spectrum (3 ms collection time + 200 ms lecture, i.e., 203 ms/frame, average spectrum obtained on 100 frames). No change was observed during these 100 frames, so that it is very unlikely that SR beam damage occurred *during* the measurement of individual XANES spectra.

However, its impact on the kinetics seems to be more indirect than the SR beam. Indeed, each sample was investigated at two different positions to test the reproducibility of the fading process. For *Anoxia* samples, the procedure consisted in inserting the sample within the environmental cell, wait 15 minutes for gas equilibration, perform the first fading experiment, change the position of the beam onto the sample and perform the second fading experiment. In other words, the sample was in anoxia respectively for 15 minutes and around 3 hours in the two successive experiments. However, no difference, neither in the kinetics nor in the starting XANES spectrum, was found between the two successive experiments (results not shown). This implies that anoxia is not the driving factor for the observed kinetics, at least in this time scale. It seems to sensitize Prussian blue to reduction, but the kinetics are mainly driven by SR beam exposure. This is confirmed by the fact that all the kinetics consist roughly in a drop of $\Delta E_a = -2$ eV after ~ 30 min whatever the environment (Fig. 3), suggesting that SR beam-induced reduction effectively governs the fading process and overcomes any other type of fading. Note that the fact that no effect of visible light could be observed does not mean that light is not a reducer of Prussian blue but that its impact is negligible compared to that of the SR beam and anoxia, in the observable time frame.

Sensitivity of Prussian blue to SR beam damage Beam damage is a major concern not only because it hinders the study of other possible factors (here light and anoxia) but also because it becomes crucial when examining precious cultural heritage samples. Schroeder et al. have already reported SR beam damage, on PB watercolor paper samples. However, those samples were conditioned in a dry Helium atmosphere [16]. Knowing the influence of humidity on Prussian blue and Prussian blue analogues [8, 11], the structure of Prussian could have already been degraded by the absence of humidity, making it artificially sensitive to SR beam exposure. For the present study, according to our results on PB-Whatman samples in *Air-Dark* (Fig. 3), it seems that our Prussian blue samples are sensitive to SR beam damage at the Fe K-edge. One strategy to avoid such a damage could consist in working with a defocused beam (typically 1 or 2 orders of magnitude more than the $30 \mu\text{m} \times 35 \mu\text{m}$ beam area used here), providing that the concentration of the sample allows one to get a sufficient signal.

Knowing the sensitivity of Prussian blue to SR beam damage, it would be very helpful to indicate, in each publication related to the analysis of historical Prussian blue by synchrotron hard X-rays, either the estimated absorbed dose of the samples or at least to mention if SR beam damage was evidenced or not. This simple check is usually performed during protein structure characterization [23] and would also

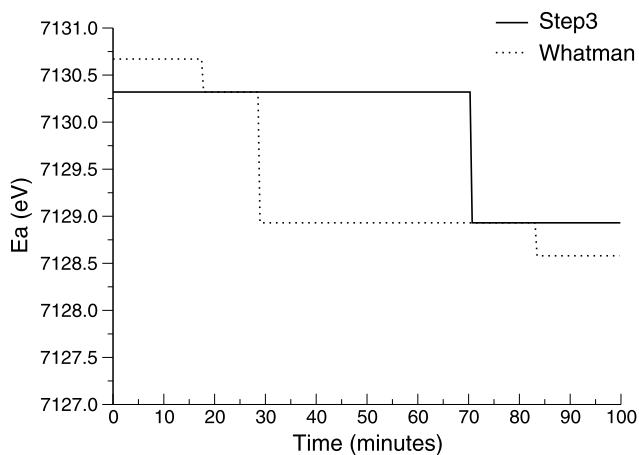


Fig. 5 $E_a(t)$ for PB-*Whatman* and PB-*Step3* samples in *Air-Dark*. For clarity, the data points have been reduced to feature only the times where E_a changes

be judicious for cultural heritage materials inherently sensitive to environmental degradation, such as organic compounds or light-sensitive pigments.

3.3 The role of the substrate

While our paper samples faded rapidly, the pigment alone is stable during long beam exposure (several hours). Therefore, the observed reduction of Prussian blue is linked with the presence nearby of the substrate. We propose here to use SR beam radiation to follow the kinetics of reduction of Prussian blue on two types of paper, namely *Whatman* and *Step3* in air. Samples were investigated in *Air-Dark*, and their reduction was induced by SR beam radiation. The kinetics seems to differ significantly between the two systems, with a main drop of E_a after ~ 30 min for PB-*Whatman* sample, but only after 70 min for PB-*Step3* (Fig. 5).

At a first glance, this result may be counter-intuitive, since *Step3* is a sensitive paper, which readily degrades. Reactive organic compounds released by the degradation could in turn react with PB, making it more prone to reduction. Several explanations can be put forward to explain such an apparent paradox: (i) the dose received by the two samples were significantly different, (ii) some components present in *Step3* paper induce a change in the kinetics, (iii) the starting crystal structure of Prussian blue was not identical on both papers, even prior to any SR beam exposure, and (iv) the spatial distribution of the pigment within the substrate is different in both paper systems.

To check hypothesis (i), we tried to estimate the dose D absorbed by the PB-paper systems upon X-ray exposure to record one average spectrum. D corresponds to the absorbed energy normalized with respect to the mass of the absorbing material irradiated [24]. Absorbed energies were

calculated based on the difference between the incident direct beam flux and the transmitted X-ray flux through the sample.³ They were estimated to be a total of a few mJ to achieve fading of PB-*Whatman* sample (30 min, 60 spectra) and PB-*Step3* sample (70 min, 140 spectra). Concerning the mass of PB irradiated, the same colloidal solution was used for preparing the samples. However, the grammages of *Whatman* and *Step3* papers are 87 and 80 gm^{-2} , respectively, and large uncertainties in the amounts of PB deposited on both paper—and thus exposed to X-ray radiation—were observed. Due to these large mass uncertainties, it becomes hardly possible to estimate correctly the effective dose D and hence conclude whether the difference in fading kinetics of Fig. 5 is inherent to the samples or due to a different dose. A change of the fading behavior with the substrate as observed here is nevertheless consistent with previous XANES and spectrophotometry measurements obtained on PB-*Whatman* and PB-*Step3* samples faded ex situ [8]. It seems therefore that even though the kinetics presented here are not fully conclusive, the two PB-paper samples seem to react differently to reduction.

The second hypothesis (ii) concerns the presence of an additional compound in *Step3*, which would inhibit PB reduction. This compound could be the lignin. Indeed, lignin is a good antioxidant and has been shown to inhibit efficiently the autoxidation of cellulose by acting as a radical scavenger [25]. We know that PB powder does not reduce easily while the same PB on *Whatman*, composed uniquely of cellulose, does. Therefore, cellulose oxidation seems to catalyze PB reduction. By mitigating cellulose degradation, lignin could thus indirectly attenuate and delay Prussian blue fading.

The third hypothesis (iii) concerns the starting crystalline structure of Prussian blue on both papers. Previous XANES studies realized on the same type of PB-paper samples have evidenced subtle changes of the structure when deposited on *Step3* paper, even without light or anoxia treatment [8]. This can be here observed on Fig. 6, where the post-edge region of the XANES spectrum at $t = 0$ min slightly differs between the two paper samples. As in previous studies, the XANES spectrum of PB on *Whatman* paper is virtually similar to that of the PB powder (results not shown). On *Step3* however, the spectrum features flatter oscillations in the post-edge region (see Fig. 6, region 7160–7200 eV) and a loss of details in the prepeak region. The exact structural features involved in these observations are for the moment unknown, but they could be sufficient to radically change the sensitivity of the pigment to fading and hence its kinetics.

The final hypothesis (iv) concerns the distribution of PB particles within the paper. This could influence the total

³An estimation of the absorbed energy, expressed in J, is: absorbed flux \times 7120 eV \times exposition time \times 1.6.10⁻¹⁹.

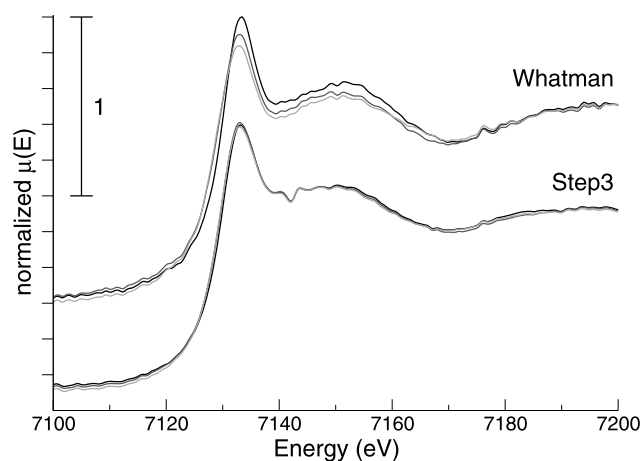


Fig. 6 XANES spectra for PB–Whatman and PB–Step3 samples in Air–Dark. Measurement times $t = 0$ min (black), $t = 20$ min (dark gray), $t = 50$ min (light gray)

available exchange interface between PB and compounds of the paper, and hence the possibilities for PB and substrate to carry out a correlated redox process. Based on similar preparation processes, we do not expect the distribution of PB to be very different in the two papers. However, this point is currently further investigated to estimate its potential influence on the final sensitivity of PB to reduction.

To conclude, presented data speak for an influence of the substrate on both the amount and the kinetics of Prussian blue fading. The exact mechanism involved is still unknown, but the various hypotheses proposed to explain the various roles of the substrate (i.e. modification of the structure of PB upon deposition and different redox properties of the substrate) shed already some light on the complex relationships between the Prussian blue structure and the substrate.

4 Conclusion

This paper demonstrates the potentiality of time-resolved X-ray absorption spectroscopy to investigate the various environmental and internal factors responsible for the fading of Prussian blue in cultural objects. Knowing the complex response of the PB structure to external stress, it is of high importance to control the environment in which PB is measured. The custom experimental setup composed of a visible light source and a flux-controlled environmental cell achieves this goal.

Its application to the investigation of Prussian blue-paper samples allowed us to estimate the relative influences of light, anoxia and SR beam on the reduction kinetics of PB. It was shown that a relatively low radiation dose was sufficient to induce PB reduction in such paper samples, warning scientists dealing with SR-investigation of precious historical PB samples about the possible risks of SR beam damage. On

the other hand, our results have also shown that the substrate could play a role on the final sensitivity of PB to reduction, so that this recommendation is difficult to generalize to other types of substrates. Similarly, anoxia was demonstrated in this paper to be a major fading source of Prussian blue. Studies are currently conducted to store and display oxygen sensitive paper-based cultural objects in anoxic frames. While this measure is likely to prevent efficiently further degradation of the paper substrate, it may lead to adversary effects for PB and other pigments sensitive to reduction [26].

Such examples of antagonism are particularly difficult to handle for conservators and raise the issue whether a conservative treatment may be optimal, that is appropriate for *all* the materials constituting the object. For scientists, it emphasizes the need to consider cultural objects as a whole, especially when the goal is to characterize the physico-chemical processes happening upon degradation. In the case of PB fading, this consists in further investigating the complex interactions between PB, substrate and environment. For that purpose, environmental cells and PB-substrate model samples have demonstrated to be invaluable tools to control and study *knowingly* both external and internal factors susceptible to influence PB fading.

Acknowledgements We would like to acknowledge Lucie Nataf of the ODE team and Frédéric Picca for his joyful and spontaneous help in python programming. Thanks also to the team of the Soleil Chemistry Laboratory for help in preparing PB-paper samples and Matjia Strlic for sharing with us interesting points on paper aging process. We thank Robert J. Koestler for suggesting us to investigate PB fading in cultural artefacts. Claire Gervais thanks the Swiss National Science Foundation for partial funding through the SNSF Professorship grant 138986. This work has been developed as part of the IPANEMA/Smithsonian Institution agreement on science cooperation.

References

1. J. Bartoll, B. Jackisch, Z. Kunsttechnol. Konserv. **21**(1), 88 (2010)
2. M. Ware, J. Chem. Educ. **85**(5), 612 (2008)
3. S. Rowe, Stud. Conserv. **49**(4), 259 (2004)
4. H.J. Buser, D. Schwarzenbach, W. Petter, A. Ludi, Inorg. Chem. **16**(11), 2704 (1977)
5. F. Herren, P. Fischer, A. Ludi, W. Halg, Inorg. Chem. **19**(4), 956 (1980)
6. M. Verdagner, Science **272**(5262), 698 (1996)
7. P.R. Bueno, F.F. Ferreira, D. Gimenez-Romero, G.O. Setti, R.C. Faria, C. Gabrielli, H. Perrot, J.J. Garcia-Jareno, F. Vicente, J. Phys. Chem. C **112**(34), 13264 (2008)
8. C. Gervais, M.A. Languille, S. Reguer, M. Gillet, E.P. Vicenzi, L. Bertrand, Submitted
9. A. Bleuzen, C. Lomenech, V. Escax, F. Villain, F. Varret, C.C.D. Moulin, M. Verdagner, J. Am. Chem. Soc. **122**(28), 6648 (2000)
10. A. Bleuzen, V. Escax, A. Ferrier, F. Villain, M. Verdagner, P. Munsch, J.P. Itie, Angew. Chem., Int. Ed. Engl. **43**(28), 3728 (2004)
11. Z.L. Lu, X.Y. Wang, Z.L. Liu, F.H. Liao, S. Gao, R.G. Xiong, H.W. Ma, D.Q. Zhang, D.B. Zhu, Inorg. Chem. **45**(3), 999 (2006)
12. M. Vidotti, S.I.C. de Torresi, J. Braz. Chem. Soc. **19**(7), 1248 (2008)

13. R. Koncki, T. Lenarczuk, A. Radomska, S. Glab, *Analyst* **126**(7), 1080 (2001)
14. L. Samain, G. Silversmit, J. Sanyova, B. Vekemans, H. Salomon, B. Gilbert, F. Grandjean, G.J. Long, R.P. Hermann, L. Vincze, D. Strivaya, *J. Anal. At. Spectrom.* **26**, 930 (2011)
15. J.M. del Hoyo-Meléndez, M.F. Mecklenburg, *Spectrosc. Lett.* **44**(2), 113 (2011)
16. S. Schroeder, N. Tsapatsaris, N. Eastaugh, in *8th European Conference on Research for Protection, Conservation and Enhancement of Cultural Heritage*, ed. by J. Kolar, Ljubljana, Slovenia, November 10–12 (2008), pp. 50–51
17. A. Dostal, G. Kauschka, S.J. Reddy, F. Scholz, *J. Electroanal. Chem.* **406**(1–2), 155 (1996)
18. A. Lerwill, J.H. Townsend, H. Liang, S. Hackney, J. Thomas, *Opt. Arts Archit. Archaeol.* **6618**, 66181G (2007)
19. F. Baudelet, Q. Kong, L. Nataf, J.D. Cafun, A. Congeduti, A. Monza, S. Chagnot, J.P. Itié, *High Press. Res.* **31**(1), 136 (2011)
20. M. Newville, *J. Synchrotron Radiat.* **8**, 322 (2001)
21. K. Hayakawa, K. Hatada, P. D'Angelo, S. Della Longa, C.R. Natoli, M. Benfatto, *J. Am. Chem. Soc.* **126**, 15618 (2004)
22. B. Cochain, D.R. Neuville, D. De Ligny, J. Roux, F. Baudelet, E. Strukelj, P. Richet, *J. Phys. Conf. Ser.* **190**, 012182 (2009)
23. J.W. Murray, E.F. Garman, R.B.G. Ravelli, *J. Appl. Crystallogr.* **37**, 513 (2004)
24. J.M. Holton, *J. Synchrotron Radiat.* **16**, 133–142 (2009)
25. J.A. Schmidt, C.S. Rye, N. Gurnagul, *Polym. Degrad. Stab.* **49**(2), 291 (1995)
26. J.H. Townsend, J. Thomas, S. Hackney, A. Lerwill, *Stud. Conserv.* **1**(Suppl.), 76 (2008)